

Published in final edited form as:

Exp Mol Pathol. 2011 April ; 90(2): 215–225. doi:10.1016/j.yexmp.2010.11.011.

Hypoxia-induced autophagic response is associated with aggressive phenotype and elevated incidence of metastasis in orthotopic immunocompetent murine models of head and neck squamous cell carcinomas (HNSCC)

Nadarajah Vigneswaran^{a,*}, Jean Wu^a, Anren Song^a, Ananth Annapragada^b, and Wolfgang Zacharias^c

^aDepartment of Diagnostic Sciences, The University of Texas Health Science Center at Houston, Dental Branch, Houston, Texas 77030, USA

^bThe University of Texas School of Biomedical Informatics at Houston, Texas 77030, USA

^cDepartments of Medicine, Pharmacology & Toxicology, James Graham Brown Cancer Center, University of Louisville, Louisville, Kentucky 40202, USA

Abstract

Hypoxia confers resistance to chemoradiation therapy and promotes metastasis in head and neck squamous cell carcinomas (HNSCC). We investigated the effects of hypoxia in tumor phenotype using immunocompetent murine HNSCC models. Balb/c mice were injected intraorally with murine squamous cell carcinoma cells LY-2 and B4B8. Intratumoral hypoxia fraction was evaluated by the immunohistochemical detection of hypoxic probe pimonidazole and carbonic anhydrase IX (CAIX). Tumor cell apoptosis and autophagy in hypoxic areas of these tumors were examined immunohistochemically. Hypoxia-induced apoptotic and autophagic responses *in vitro* were examined by treating LY2 cells with CoCl₂. B4B8 tumors exhibited a non-aggressive phenotype characterized by its slow growth rate and the lack of metastatic spread. LY2 tumors demonstrated an aggressive phenotype characterized by rapid growth rate with regional and distant metastasis. Intratumoral hypoxia fraction in B4B8 tumors was significantly lower than LY2 tumors. Hypoxic areas in B4B8 tumors exhibited increased apoptosis rate than LY2 tumors. In contrast, hypoxic areas in LY2 tumors revealed autophagy. Induction of hypoxia *in vitro* elicited autophagy and not apoptosis in LY2 cells. Induction of autophagy coupled with blockage of apoptosis in hypoxic areas promotes tumor cells survival and confers aggressive phenotype in immunocompetent murine HNSCC models.

© 2010 Elsevier Inc. All rights reserved.

*Corresponding author, Department of Diagnostic Sciences, The University of Texas Health Science Center at Houston, Dental Branch, 6516 M.D. Anderson Blvd; DB 3.094G, Houston, Texas 77030, USA, Tel: 713-500-4410, Fax: 713-500-4416, nadarajah.vigneswaran@uth.tmc.edu.

Publisher's Disclaimer: This is a PDF file of an unedited manuscript that has been accepted for publication. As a service to our customers we are providing this early version of the manuscript. The manuscript will undergo copyediting, typesetting, and review of the resulting proof before it is published in its final citable form. Please note that during the production process errors may be discovered which could affect the content, and all legal disclaimers that apply to the journal pertain.

Conflict of Interest Statement:

The authors declare that there are no conflicts of interest.

Keywords

Head and neck squamous cell carcinoma; Tumor model; Hypoxia; Apoptosis; Autophagy; Carbonic anhydrase IX; Pimonidazole

Introduction

Head and neck squamous cell carcinoma (HNSCC) is the sixth most common malignancy worldwide with an estimated annual incidence of 500,000 cases (Parkin et al., 1999). The current 5-year survival rate for HNSCC is less than 50% which has remained unchanged during the last five decades (Mashberg, 2000). By the time diagnosis is made, approximately two-thirds of HNSCC patients have locally advanced disease (stages III or IV); their prognosis is extremely poor, with an estimated survival rate of 30% (Forastiere et al., 2001; Haddad and Shin, 2008; Seiwert and Cohen, 2005). Poor survival in these patients is attributable to persistent or recurrent disease (Day and Blot, 1992; Seiwert and Cohen, 2005). Patients with locally advanced HNSCC are treated primarily with radiation therapy (RT) alone or in combination with surgery and/or chemotherapy (Eisbruch et al., 2001; Forastiere et al., 2001; Fu, 1997; Haddad and Shin, 2008; Kyasa et al., 2008; Lorch et al., 2008; Marur and Forastiere, 2008; Pignon et al., 2000). A critical limit for the effectiveness of radio- and chemotherapy in HNSCC is the presence of intratumoral hypoxic areas (Brizel et al., 1997; Janssen et al., 2005; Le, 2007; Peters, 2001; Vordermark and Brown, 2003). Most solid malignant tumors including HNSCC develop chronic or transient reduction in oxygen tension below physiological levels (hypoxia). Intratumoral hypoxia, which plays a causative role in the development of metastatic disease, is a common feature in human HNSCC (Chaudary and Hill, 2007; Evans et al., 2000; Janssen et al., 2005; Koshikawa et al., 2006; Nordmark et al., 2005; Rofstad et al., 2007; Sullivan and Graham, 2007; Wijffels et al., 2008; Zhang and Hill, 2004). Moreover, hypoxia induces an immunosuppressive tumor microenvironment and protects tumor cells from anti-tumor immunity via diverse mechanisms (Le et al., 2005; Lukashev et al., 2007; Siemens et al., 2008). However, little is known how hypoxia-induced changes in the tumor microenvironment influence the host's anti-tumor immune responses in HNSCC. This potential for hypoxia-mediated suppression of host anti-tumor immunity clearly warrants a thorough investigation in order to further develop effective cancer treatment targeting hypoxia in HNSCC. In this article we describe the establishment of orthotopic murine HNSCC models with an intact immune system that might be useful for preclinical testing of hypoxia-targeted tumor imaging and therapies.

Most of the previously reported orthotopic preclinical models of HNSCC utilize immunodeficient mice into which human HNSCC xenografts are transplanted (Bozec et al., 2008; Dinesman et al., 1990; Henson et al., 2007; Mognetti et al., 2006; Myers et al., 2002; Qiu et al., 2003; Sano and Myers, 2009). The lack of a competent immune system in these mouse models may not accurately recreate the hypoxia-related tumor phenotype and progression of human HNSCC because immune-mediated constraints on tumor progression involve both the innate and acquired immune system (Shankaran et al., 2001; Swann et al., 2008). Another important consideration for mouse models of HNSCC that have intact immunity involves testing the therapeutic efficacy of tumor antigen-targeted humanized monoclonal antibodies. Humanized monoclonal antibody-based therapy is becoming an important component of targeted therapy against solid malignancies (Yan et al., 2008). Interestingly, recent studies suggest that host anti-tumor immune responses play critical roles in the clinical response to monoclonal antibody therapy (Lopez-Albaitero and Ferris, 2007; Reusch et al., 2006).

Therefore, development of an orthotopic immunocompetent mouse model of HNSCC is critical to further our understanding of the mechanisms by which hypoxia promotes HNSCC metastasis and therapeutic resistance. This, in turn, can aid in developing new pharmacologic strategies to manipulate tumor hypoxia for therapeutic benefit. The purpose of the present study is to develop syngeneic orthotopic murine models of non-metastatic and metastatic HNSCC that parallel the clinical and biologic behaviors of human HNSCC and characterize the effects of tumor hypoxia on these tumor models..

Materials and methods

Tissue culture and cell lines

Murine squamous cell carcinoma (SCC) cell lines PAM-LY (LY-2) and B4B8-Scid (B4B8) were as monolayers in Ham's F12: DME medium (1:1) supplemented with 2mM L-glutamine, 100 µg/ml penicillin G, 100 µg/ml streptomycin, 0.25 µg/ml amphotericin B and 10% fetal calf serum (Life Technologies) at 37 °C with 5% CO₂. The LY-2 cell line was isolated from lymph node metastases that developed in BALB/c mice after inoculation of PAM 212 squamous cell carcinoma cells (Chen et al., 1997). The parental PAM 212 was derived from neonatal BALB/c epidermal keratinocytes which were spontaneously transformed *in vitro* and were tumorigenic in athymic nude Balb/c congenic mice (Yuspa et al., 1980). B4B8 is a murine SCC cell line derived from BALB/c oral keratinocytes treated with chemical carcinogen 4NQO (Thomas et al., 1999).

Reagents

Antibody against carbonic anhydrase IX (CA-IX) was obtained from Abcam (Cambridge, MA); antibodies against proliferating cell nuclear antigen (PCNA) and cyclin D1 were obtained from Santa Cruz Biotechnology, Inc. (Santa Cruz, CA); antibody specific for mouse cathepsin B was obtained from Upstate (Lake Placid, NY); antibodies specific for cleaved caspase 3 (casp-3) and Beclin-1 were obtained from Cell Signaling Technology, Inc. (Danvers, MA). Mouse monoclonal antibody against β-actin was obtained from Sigma-Aldrich Co (St. Louis, MO). Streptavidin-Alexa Fluor® 488 was obtained from Molecular Probes (Invitrogen, Carlsbad, CA). The Hypoxypobe-1™ Kit consisting of pimonidazole (Hypoxypobe-1) and a mouse monoclonal antibody against pimonidazole adducts was obtained from Chemicon International (Temecula, CA). The DAKO ARK (Animal Research Kit)-peroxidase, biotinylated goat anti-rabbit/mouse immunoglobulins, EnVision+ System-horseradish peroxidase (HRP) and -alkaline phosphatase (AP) kits were obtained from DakoCytomation (Carpenteria, CA).

Animal tumor models

All protocols for animal tumor models were approved by the Institutional Animal Care and Use Committee of the University of Texas Health Science Center at Houston. Six-week-old female BALB/c mice were purchased from Harlan (Indianapolis, IN). B4B8 and LY2 cells were grown to 75% confluence and harvested and resuspended in phosphate buffered saline (PBS). Cell suspensions were mixed with equal volumes of Matrigel (BD Biosciences, San Jose, CA) and injected sub-mucosally via intraoral route into the right buccal sulcus at a final concentration of $1 \times 10^6/0.1\text{ml}$ per animal. Tumor sizes were measured weekly and tumor volumes were estimated using the formula ($V = A \times B^2/2 \text{ mm}^3$), where A and B are the longer and shorter diameters of the swelling. We monitored the mice with tumors daily and mice exhibiting signs of morbidity according to the guidelines set by the Institutional Animal Care and Use Committee were sacrificed immediately. Mice were euthanized by exsanguination under isoflurane anesthesia and then primary tumors, regional lymph nodes and lungs were harvested. These tissues were fixed in 10% neutral buffered formalin, embedded in paraffin and serial sections were made and used for hematoxylin and eosin

staining and for immunohistochemical studies. All immunohistochemical analyses were conducted on the primary tumor sections.

Detection of tumor hypoxia

Hypoxypobe-1™ (Pimonidazole hydrochloride) was injected into the tail vein of the mice (60mg/Kg = 1.5 mg in 100 µl of 0.9% NaCl per mice) two hours prior to sacrificing the animal. Immunohistochemical detection of pimonidazole adducts formed within the intratumoral hypoxic areas were examined using the anti-pimonidazole antibody. Tissue sections were deparaffinized, rehydrated and subjected to antigen retrieval by boiling in ANTIGEN *DECLOAKER* (Biocare Medical, Concord, CA, USA). Endogenous peroxidase activity was blocked with 3% H₂O₂ in methanol. Tissue sections were incubated with monoclonal mouse anti-pimonidazole antibody (Hypoxypobe-1 MAb; 1: 50) that had been previously biotinylated followed by addition of Streptavidin-HRP (DAKO ARK). CA-IX was used as an endogenous marker for tumor hypoxia. CA-IX expression in tumor sections was examined using a polyclonal rabbit anti-CA-IX antibody (1:1000). CA-IX antibody immunoreactive sites were detected with EnVision+ System-horseradish peroxidase (HRP) kit for rabbit primary antibodies according to the manufacturer's instruction.

Immunohistochemical analyses of tumor cell proliferation, apoptosis and autophagy

Markers of cell proliferation, apoptosis and autophagy in primary B4B8 (n=5) and LY2 tumors (n=5) were examined by immunohistochemistry. Representative tumor sections were deparaffinized and rehydrated and antigen retrieval was performed by boiling in ANTIGEN *DECLOAKER* (Biocare Medical, Concord, CA, USA) solution for two minutes. Endogenous peroxidase activity was quenched by incubating the tissue section with 3% H₂O₂ in methanol for ten minutes. Non-specific binding sites were blocked by incubating the tumor sections in BACKGROUND *TERMINATOR* (Biocare Medical, Concord, CA, USA) solution for ten minutes. Proliferation rates of these tumors were examined with mouse monoclonal anti-PCNA (1:100) and anti- cyclin D1 (1:50) antibodies. Apoptosis and autophagic responses in hypoxic areas of the tumors were examined using the rabbit polyclonal anti-mouse cathepsin B antibody (1:100), rabbit monoclonal anti-casp-3 (1:100) and rabbit polyclonal anti-Bec-1(1:100) antibodies. Immunoreactivity of mouse monoclonal antibodies (PCNA and cyclin D1) was detected using the DAKO ARK according to the protocol provided with this kit. We used EnVision®+ System-HRP kit and its recommended protocol for detection of rabbit monoclonal (caspase 3) and polyclonal (cathepsin B and Beclin 1) antibody binding sites. We used Animal Research Kit-HRP and EnVision®+ alkaline phosphatase (AP) kit for simultaneous detection of pimonidazole and cathepsin B, respectively, in tumor sections. HRP and AP reactive sites in tissue sections were visualized using diaminobenzidine tetrachloride and Fast Red as chromogenic substrates, respectively. For negative controls, non-immune mouse or rabbit serum was substituted instead of mouse or rabbit primary antibodies, respectively.

In vitro detection of autophagy in LY2 cells under hypoxia-mimetic conditions

Cobalt chloride (CoCl₂) treatment of cells *in vitro* activates hypoxia signaling by stabilizing HIF1 α and induces cellular changes which are identical to those seen after hypoxia (Bunn and Poyton, 1996; Goldberg and Schneider, 1994; Piret et al., 2004). Sub-confluent cultures of LY2 cells were washed twice with PBS and hypoxia-like conditions were chemically created by incubating the cells in culture medium containing 250 µM CoCl₂ for 24–48 hr. At the end of the treatment, adherent and floating cells were harvested and lysed by M-PER™ mammalian protein extraction reagent (PIERCE, Rockford, IL) supplemented with Complete Protease Inhibitor Cocktail (Roche Applied Sciences, Indianapolis, IN). The cell lysates (20 µg) were subjected to electrophoresis on a 4–20% Tris-Glycine SDS-PAGE (Invitrogen, Carlsbad, CA), followed by transfer to a nitrocellulose membrane using the

iBlot™ Dry Blotting system (Invitrogen). The blot was probed with rabbit anti-Beclin-1 antibody (1:1000) followed by HRP-conjugated goat anti-rabbit antibody (Pierce,) and chemiluminescence detection. The same blot was re-probed using monoclonal mouse anti-β actin (1:5000) antibody after stripping with BlotFresh™ Western blot stripping reagent (SignaGen® Laboratories, Gaithersburg, MD). For immunohistochemical detection of autophagy, LY2 cells were grown in microscopic slide chambers for 50–60% confluence and then treated with CoCl₂ for 48 hr. At the end of treatment cells were fixed in 2% paraformaldehyde for immunohistochemical detection of autophagic marker Beclin-1. LY2 cells treated with CoCl₂ and non-treated control cells were probed with polyclonal rabbit anti-Beclin-1 (1:100) and its immunoreactivity was demonstrated using the EnVision®+ System-HRP kit according to the manufacturer's instructions.

Image and data analyses

Computerized image analyses of immunostained primary tumor sections were performed using the Image-Pro Plus 5.1 program. Quantification of hypoxia fraction identified by either pimonidazole binding or by CA-IX expression was performed at low magnification. Digital photomicrographs of the entire primary tumor areas were acquired using a SPOT digital camera (Diagnostic Instruments Inc. Sterling Heights, MI, USA). Using image analysis software (Image-Pro Plus 5.1) pimonidazole-positive, CA-9 positive areas and the total areas of the primary tumor sections were determined. The hypoxia fraction (%) was defined as pimonidazole- or CA-IX positive area/total tumor areas × 100. Ten representative tumors were examined for each tumor type (B4B8 and LY2). Proliferative activity of these tumors was determined by counting PCNA/cyclin D1-positive nuclei in randomly selected high-power fields (HPF; n=5). The number of PCNA/cyclin D1-positive cells per HPF was recorded as their respective labeling indices (LI) for each tumor type. Tumor cell apoptosis in hypoxic areas (n=5; as determined by pimonidazole binding) was examined by immunolabeling for cleaved casp-3. Apoptosis rates of tumor cells in hypoxic areas were defined as number of casp-3 positive cells per HPF. All statistical analyses were performed using GraphPad Prism 4 and *p*-values less than 0.05 were considered to be statistically significant.

Results

Biologic behaviors of orthotopic oral cancer models

Implantation of murine SCC cell lines LY2 and B4B8 within the mandibular buccal sulcus of syngeneic BALB/c mice formed tumors in 100% and 85% of the mice, respectively (Figures 1 & 2). LY2 tumors became grossly identifiable within one week post implantation and grew rapidly to produce a mean tumor volume of $36.4 \pm 10.8 \text{ mm}^3$ within 3 weeks (Figure 3). Accompanying this rapid tumor growth, the tumor bearing mice exhibited cachexia and needed to be sacrificed within the 25th day postinoculation of tumor cells. On the other hand, growth rate of B4B8 tumors was slow and the tumors could be grossly identified only two weeks after inoculation (Figure 3). B4B8 tumors reached a mean volume of $17.7 \pm 2.2 \text{ mm}^3$ 6 weeks post implantation; the B4B8 tumor bearing mice did not exhibit cachexia or any other tumor-related distress 8 weeks after tumor cell implantation (Figure 3). The results indicated that the clinical behavior of LY2 tumors was more aggressive than B4B8 tumors.

Histopathologic findings

Hematoxylin and eosin stained serial sections of primary tumors, regional lymph nodes; lung and liver tissue were used for histopathologic examination. Primary tumors of B4B8 and LY2 were located underneath the mucosal epithelium invading deeply into the skeletal muscle, mandible and adjacent salivary gland lobules (Figure 4). Histologic and cytologic

features of primary B4B8 tumors were compatible with a well to moderately differentiated squamous cell carcinoma (Figure 4 A–C). B4B8 tumors revealed invasive islands and cords of malignant squamous epithelial cells with abundant eosinophilic cytoplasm and uniformly sized hyperchromatic nuclei (Figure 4 A–C). The mitotic activity of this tumor was low (3–5/HPF) without any abnormal mitotic activity. Perineural or vascular invasion was not present. The primary LY2 tumors revealed histologic and cytologic features of a poorly differentiated basaloid squamous cell carcinoma (Figure 4 D–F). LY2 primary tumors were composed of sheets of basaloid poorly differentiated large polygonal and ovoid malignant epithelial cells with pleomorphic and hyperchromatic nuclei containing multiple prominent nucleoli (Figure 4 D–F). Frequent perineural invasion was noted with most LY2 primary tumors. LY2 tumor cells exhibited a high mitotic index (12–15/HPF) with atypical mitosis. LY2 tumors demonstrated multifocal satellite necrosis comprising 10% to 25% of the total tumor area. The incidence of regional lymph node metastasis was 91% (33/36) and distant lung metastasis was 32% (11/36) with LY2 tumors (Figures 2 & 5). There was no evidence of nodal or lung metastasis with B4B8 tumors. Neither LY2 nor B4BD tumors had liver metastases or any other distant metastases.

Proliferation rate of orthotopic B4B8 and LY2 tumors

We used the PCNA and cyclin D1 labeling indices to measure the proliferation rate of B4B8 and LY2 tumors (Figure 6). PCNA and cyclin D1 immunoreactivity was localized mostly in nuclei of tumor cells with a weak cytoplasmic reactivity in some tumor cells (Figure 6). Tumor proliferation rate measured by PCNA labeling index was significantly ($p < 0.0001$) lower in B4B8 tumors (range =146–367; mean \pm SEM = 257 ± 33.6) compared to LY2 tumors (range =583–937; mean \pm SEM = 758.2 ± 46.0). Cyclin D1 labeling index was also lower in B4B8 tumors (range =68–155; mean \pm SEM = 126.5 ± 15.4) than LY2 tumors (range =92–268; mean \pm SEM = 176.2 ± 21.7), however the difference was not statistically significant ($p = 0.117$).

Hypoxic areas in B4B8 and LY2 tumors

Hypoxic areas in these tumors were identified by their positive immunostaining for CA-IX and pimonidazole (Figure 7). Hypoxic tumor cells exhibited a strong cell membrane and a weak cytoplasmic staining for CA-IX and revealed an intense cytoplasmic staining for pimonidazole. Hypoxic areas were detected in 100% (20 of 20) and 70% (14 of 20) of LY2 and B4B8 tumors, respectively. On average, the hypoxic area is significantly higher in LY2 primary tumors than B4B8 tumors. Both pimonidazole and CA-IX positive tumor cells were frequently noted in peri-necrotic areas; however, the hypoxic tumor fractions identified by CA-IX staining were significantly greater than tumor fractions identified by pimonidazole binding (Figure 7). Moreover, there were areas of mismatch in both B4B8 and LY2 tumors where CA-IX positivity was found without pimonidazole binding but not *vice versa*.

Hypoxia-induced apoptotic and autophagic responses in B4B8 and LY2 tumors

Apoptotic cells positive for cleaved casp-3 were detected in abundance in hypoxic areas of B4B8 tumors, whereas hypoxic areas in LY2 tumors were essentially negative for casp-3 (Figure 8). Hence, the tumor hypoxia-related apoptotic rate was significantly higher ($p < 0.001$) in B4B8 tumors (26.6 ± 10.92 /HPF) compared to LY2 tumors (6.2 ± 1.4) (Figure 8). In B4B8 tumors, the apoptosis was localized to discrete, patchy areas, which in most cases corresponded to the hypoxic areas. In contrast, hypoxic areas of LY2 tumor demonstrated patchy areas of necrosis, essentially devoid of apoptotic tumor cells. Moreover, hypoxic areas in LY2 tumors demonstrated overexpression of autophagy-regulating protein Beclin-1 in viable tumor cells found in the peri-necrotic areas (Figure 9) (Cao and Klionsky, 2007). Lysosomal protease cathepsin B, which participates in both apoptosis and autophagy, was also overexpressed in hypoxic areas of LY2 tumors (Vigneswaran et al.,

2005; Wickramasinghe et al., 2005; Yan et al., 2005). Extending this observation, we performed double immunolabeling and confirmed up-regulation cathepsin B expression in hypoxic areas compared to normoxic areas of LY2 tumors. Increased expression of cathepsin B in hypoxic LY2 tumor cells was noted in large granules consistent with phagolysosome (Figure 9).

Chemically induced hypoxia up-regulates the expression of autophagy-regulatory protein Beclin 1

Cobalt chloride (CoCl₂), a chemical inducer of HIF-1, is frequently used as an *in vitro* mimic of hypoxia in cells because it induces biochemical and morphological changes similar to those seen after hypoxia (Bunn and Poyton, 1996; Goldberg and Schneider, 1994; Piret et al., 2004). Hypoxia was induced in LY2 cells by treating them with CoCl₂ for 24 and 48 hr and their Beclin 1 protein levels were examined by immunoblotting and immunohistochemistry. Hypoxia-induction in LY2 cells by CoCl₂ treatment caused an increase in Beclin-1 protein level (Figure 10). CoCl₂ treatment increased the expression levels of Beclin-1 but not cleaved casp-3 in LY2 cells (Figure 11).

Discussion

We describe two orthotopic models of HNSCC in immunocompetent mice representing low-grade non-metastatic (B4B8) and high-grade metastatic (LY2) HNSCC. Histopathologic features of B4B8 tumors closely resemble a low-grade, well-differentiated HNSCC. These tumors revealed slow growth rate and local invasion but no regional or distant metastasis. In contrast, LY2 tumors revealed aggressive growth with high rates of locoregional and distant metastases. LY2 tumors demonstrated histopathologic features of a high-grade poorly differentiated HNSCC, characterized by increased and abnormal mitotic figures, marked cellular and nuclear pleomorphism and multifocal necrosis. We examined the proliferative activity of LY2 and B4B8 tumors by PCNA immunolabeling studies, which revealed that proliferative activity of LY2 tumors is significantly higher than the B4B8 tumors. Cyclin-D1, a major regulator of cell proliferation, is also overexpressed in LY2 tumors compared to B4B8 tumors. This finding is in accordance with the published reports that increased expression of cyclin D1 in human HNSCC is associated with poor prognosis and increased risk for metastasis (Capaccio et al., 2000; Yu et al., 2005).

HNSCC xenograft models were initially developed by implanting human-derived HNSCC cells subcutaneously into athymic nude mice and severely combined immunodeficient mice. These models are used to evaluate the *in vivo* tumorigenic capacity of human-derived HNSCC cells and for pre-clinical testing of anticancer agents against human HNSCC (Sano and Myers, 2009). These subcutaneous models are preferred to test the efficacy of anti-cancer therapies because these tumors are easy to establish, monitor and measure reproducibly (Sano and Myers, 2009). However, they fail to mimic the local growth patterns and metastatic pathways of HNSCC and hence preclinical studies performed using these models failed to predict the therapeutic efficacy of anticancer agents in human HNSCC (Sano and Myers, 2009).

On the other hand, orthotopic mouse models of HNSCC, in which tumor cells growing in their natural location closely simulate the primary tumor site microenvironment, and reproduce local growth as well as the regional and distant metastatic spread of human HNSCC with high fidelity (Sano and Myers, 2009). Moreover, orthotopic HNSCC models produce a higher rate of spontaneous tumor metastasis than subcutaneous xenograft models (Sano and Myers, 2009). However, most of these orthotopic models of HNSCC were established using immunodeficient mice into which human HNSCC cells were implanted either into the tongue or floor of the mouth (Sano and Myers, 2009) These HNSCC

xenograft mouse models do not faithfully recreate the complex interactions between tumor cells and host immunity that occur during the local growth, regional and distant metastasis. In contrast, the orthotopic HNSCC models described in this study involve immunocompetent mice and the tumors have histologic appearances and patterns of disease progression similar to low and high-grade human HNSCC.

Tumor microenvironment plays a critical role in determining the therapeutic response of solid tumors (Liotta and Kohn, 2001; Tredan et al., 2007). Intratumoral hypoxia, a common characteristic of solid malignancies, is an important component of the tumor microenvironment. Hypoxia was suggested to contribute to the aggressive phenotypes of head and neck cancer, with large tumor size, high histologic grade, high proliferation rate and locoregional spread (Aebersold et al., 2001; Isa et al., 2006; Nordmark et al., 2005; Pitson et al., 2001; Vordermark and Brown, 2003). Hence, we evaluated the extent of intratumoral hypoxia in these two phenotypically distinct HNSCC models.

A number of different methods have been used to assess the oxygenation status of solid tumors *in vivo*. Oxygenation status of solid tumors can be measured in real-time using oxygen electrodes inserted into the tumor (Brizel et al., 1997). Nitroimidazole-based reagents such as pimonidazole undergo a nitroreductase catalyzed single-electron reduction, and bind covalently to cellular components in hypoxic cells (Bennewith et al., 2002). Bound compounds can be detected immunohistochemically or radiolabeled for positron emission or single photon emission computer tomographic imaging studies (Chapman et al., 1998). Expression levels of intrinsic markers of hypoxia are also widely used to determine the hypoxic status of solid malignant tumors (Vordermark and Brown, 2003). Hypoxia induces the expression and stabilization of hypoxia-inducible factor-1 α (HIF-1 α) which in turn up-regulates numerous HIF1-dependent genes which include CA-IX (Vordermark and Brown, 2003). CA-IX, a transmembrane glycoprotein, regulates pH by reversible hydration of carbon dioxide to carbonic acid and is critical for neutralizing hypoxia-related acidification caused by a glycolytic switch in hypoxic tumor cells. CA-IX, which is overexpressed in solid malignancies, reveals strong inverse correlation with intratumoral oxygen tensions, is widely used as an intrinsic marker for tumor hypoxia. CA-IX over-expression in human HNSCC is associated with poor prognosis (Beasley et al., 2001; Roh et al., 2009).

In this study, we used both pimonidazole adduct formation and CA-IX expression patterns to determine the extent of hypoxia in B4B8 and LY2 tumors. Our data showed hypoxic areas as measured by immunostaining for both pimonidazole and CA-IX are significantly higher in LY2 primary tumors compared B4B8 tumors. Intratumoral hypoxia levels are markedly higher in high-grade LY2 primary tumors with metastatic phenotype than non-metastatic B4B8 tumors. Our finding is in line with the published reports that patients with severely hypoxic tumors have greater risk of developing regional and distant metastases than patients with normoxic tumors (Sullivan and Graham, 2007).

It should be noted that many of the hypoxic areas in LY2 tumors were concentrated around areas of necrosis and in these areas both markers were co-localized. Hypoxic areas as detected by CA-IX staining were larger in both tumor types than hypoxic areas delineated by pimonidazole binding. Although both markers co-localized in hypoxic areas of some tumors, there were areas of mismatch between both markers in other tumors. This mismatch was more remarkable in B4B8 tumors than LY2 tumors. Our data suggest that CA-IX expression in B4B8 is probably also mediated by hypoxia-independent signaling pathways.

Most solid malignant tumors, including head and neck cancers, exhibit areas of hypoxia that are heterogeneously distributed within the tumor mass (Brizel et al., 1997; Brown and Giaccia, 1998; Harris, 2002; Isa et al., 2006; Janssen et al., 2005). Structural and functional

abnormalities of tumor microvessels (perfusion-limited oxygen delivery) and an increase in diffusion distances (diffusion-limited oxygen delivery) are responsible for the development of acute and chronic hypoxia, respectively, in rapidly growing malignant tumors (Vaupel and Mayer, 2007). Hypoxia is known to promote genetic instability among tumor cells and to confer on them a more malignant phenotype leading to aggressive tumor growth, regional and distant metastasis and poor patient survival (Bristow and Hill, 2008). Hypoxia induces genetic instability in surviving tumor cells by decreasing DNA repair and by increasing mutation rate and hence provides a selective pressure for the expansion of more aggressive and metastatic tumor cell population (Koshikawa et al., 2006).

Hypoxia-mediated signaling in tumor cells up-regulate the expression of stem cell-specific genes and promote the maintenance of cancer stem cells (Kim et al., 2009). Moreover, tumor hypoxia causes resistance to radiation therapy and reduces the efficacy of chemotherapy and immunotherapy (Brizel et al., 1997; Cao et al., 2007; Chapman et al., 1998; Cuisnier et al., 2003; Nordmark et al., 1996; Pouyssegur et al., 2006). Hence, hypoxia is a major impediment for successful treatment of locally advanced head and neck cancers and is considered to be a critical target for developing effective anticancer agents (Janssen et al., 2005; Peters, 2001). Hypoxia-inducible factor (HIF), a heterodimeric transcription factor, is activated and stabilized in tumor cells in response to reduced oxygen tension. HIF plays an important role in tumor progression by upregulating genes that promote angiogenesis, metastasis and resistance to oxidative stress (Chaudary and Hill, 2007; Rofstad et al., 2007). It also regulates the switch to anaerobic metabolism which is critical for tumor cell survival under hypoxia. Tumor hypoxia also modulates tumor-host stroma interaction and specifically enhances immune privilege of tumor cells by suppressing host immune surveillance (Le et al., 2005).

Hypoxia exerts dual responses in tumors, by mediating either tumor cell apoptosis or survival, depending on whether or not the apoptotic pathway of tumor cells is intact (Kilic et al., 2007). Hence, we evaluated tumor cell apoptosis as identified by immunolabeling for cleaved caspase-3 in hypoxic areas of B4B8 and LY2 tumors. B4B8 tumors revealed an increased rate of apoptosis in hypoxic areas compared to normoxic areas. On the other hand, hypoxic areas in LY2 tumors were negative for cleaved caspase-3 positive apoptotic cells. Tumor cells successfully adapting to the hypoxic environment have significant proliferation and survival advantage leading to an aggressive phenotype. Our findings suggest that hypoxia induces apoptosis in non-aggressive B4B8 tumors but not in highly aggressive LY2 tumors. It appears that in LY2 tumors, hypoxia facilitates clonal selection of tumor cells having resistance to apoptosis (Carmeliet et al., 1998). Hypoxia is reported to induce cell cycle arrest in some tumors leading to chemo-radiation resistance of tumor cells, including oral cancer cells (Goda et al., 2003; Wijffels et al., 2008). However, hypoxia does not appear to induce cell cycle arrest in LY2 tumors because there were no remarkable differences in the PCNA and Cyclin D labeling indices between hypoxic and normoxic areas of these tumors.

We examined the expression patterns of Beclin-1 and cathepsin B, molecules implicated in autophagy in the hypoxic and normoxic areas of B4B8 and LY2 tumors (Cao and Klionsky, 2007; Yan et al., 2005). Hypoxic areas of LY2 tumors but not those of B4B8 tumors expressed increased levels of Beclin-1 and cathepsin B compared to the normoxic areas of the same tumor. Our data suggest that autophagy may play a protective role in LY2 tumors by delaying hypoxia-induced apoptosis. Previous studies have shown that elimination of damaged mitochondria by autophagy prevented the release of pro-apoptotic signaling molecules from mitochondria leading to the inhibition of apoptotic cell death (Eisenberg-Lerner et al., 2009). It is noteworthy that hypoxic areas of LY2 tumors express markers of autophagy (Beclin-1 and cathepsin B) but not apoptosis (cleaved casp-3).

In solid malignant tumors, autophagy can be activated in response to hypoxia as a survival mechanism in conditions of nutrient deprivation (Azad et al., 2008). Furthermore, hypoxia-induced autophagy contributes to tumor cell resistance to anticancer drugs (Song et al., 2009). Autophagy (self-eating) is usually activated by nutrient deprivation under ischemia and is essential for cell adaptation to adverse environment (Levine and Kroemer, 2008). During autophagy, cells engulf portions of the cytosol and cytoplasmic organelles within double- or multi-membraned autophagosomes and deliver them to lysosomes for degradation. Autophagy not only allows the cells to recycle amino acids but also facilitates the removal of damaged cytoplasmic organelles. Occurrence of autophagy in solid tumors as a response to metabolic stress has been reported but its role in tumor biology has been contradictory (Dalby et al.). Partial inactivation of the autophagic response due to heterozygous deletion of Beclin-1, the mammalian homolog of the yeast autophagy gene *ATG6*, has been shown to increase the incidence of spontaneous malignancies (Qu et al., 2003). These findings support the notion that autophagy can suppress tumorigenicity through initiation of a specific type of programmed cell death (Dalby et al., 2010). On the other hand, autophagy may work in favor of cancer cells by protecting them against harsh any tumor microenvironment (Dalby et al., 2010). Indeed, certain cancer cells exploit autophagy as a pro-survival mechanism to adapt to hypoxia- and therapeutically-induced cell stress or damage (Pursiheimo et al., 2009; Song et al., 2009).

We also addressed whether we can demonstrate an autophagic response in LY2 cells which are exposed to hypoxia *in vitro* using the hypoxia-mimetic agent cobalt chloride (CoCl₂) (Fu et al., 2009; Karovic et al., 2007). We show that the expression of autophagic marker Beclin-1 was increased after CoCl₂-induced hypoxia in LY2 cells. These results imply that autophagy response in LY2 cells is an adaptation to the hypoxic and metabolically stressed environment. Our findings suggest that in LY2 tumors, cells in hypoxic areas undergo necrosis, however some of them survive in a dormant state and restart to proliferate when new vasculature reach the hypoxic area. Interestingly, reoxygenation, due to the neovascularization increases the metastatic ability of cancer cells which may explain the highly metastatic phenotype of LY2 tumors (Subarsky and Hill, 2003). Strikingly, it was recently reported that hypoxia induces overexpression of Beclin-1 in nasopharyngeal and colorectal carcinomas which is associated with aggressive clinical behavior and poor prognosis (Koukourakis et al., 2010; Wan et al., 2010).

Conclusions

The mouse models of HNSCC described in this study have significant advantage over the previously reported HNSCC xenograft models in which tumor microenvironment does not faithfully reproduce human HNSCC. Further, our data demonstrated that hypoxia induces differential responses in non-aggressive (B4B8) and aggressive (LY2) HNSCC models. Our data suggest that induction of autophagy coupled with blockage of apoptosis in hypoxic areas promotes tumor cells survival and confers aggressive phenotype in HNSCC. These orthotopic HNSCC models would be valuable to study the hypoxia- and autophagy-targeted anticancer therapies and their effect in the tumor microenvironment.

Abbreviations

HNSCC	head and neck squamous cell carcinoma
PCNA	proliferating cell nuclear antigen
4NQO	4-Nitroquinoline 1-oxide
CA-IX	carbonic anhydrase IX

SCC	squamous cell carcinoma
HPF	high power field
HRP	horseradish peroxidase
AP	alkaline phosphatase
SEM	standard error of mean
Casp-3	caspase 3

Acknowledgments

We thank Dr. Carter Van Waes (NIDCD/NIH) and Dr Giovana R. Thomas (Department of Otolaryngology Head and Neck Surgery, University of Miami School of Medicine) for providing us the murine SCC cell lines LY2 and B4B8 cells, respectively. This work was supported by NIH/NIDCR grants DE13150 (W.Z); RO3 DE15723 (N.V) and R21DE019956 (N.V).

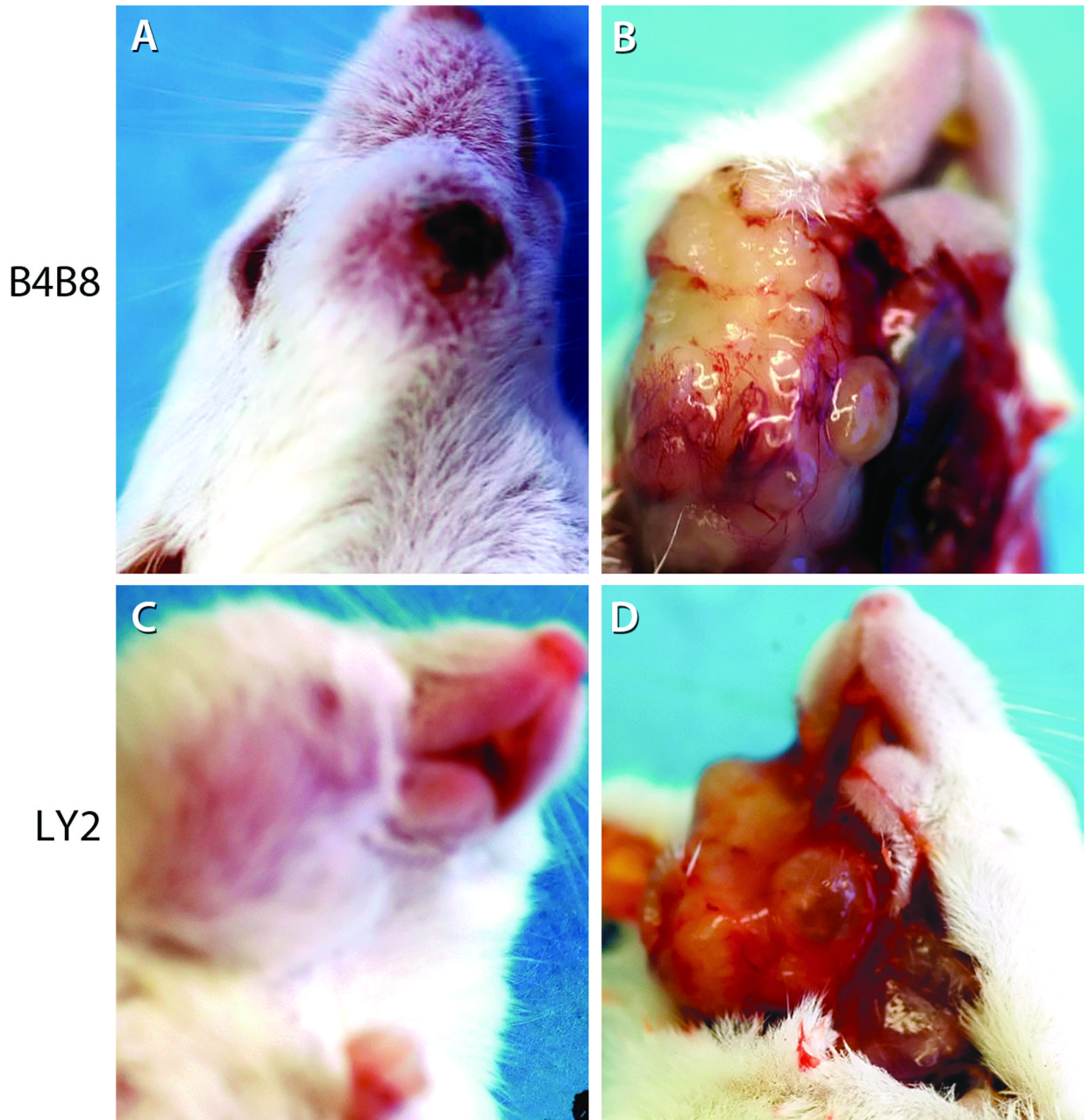
References

- Aebersold DM, et al. Expression of hypoxia-inducible factor-1alpha: a novel predictive and prognostic parameter in the radiotherapy of oropharyngeal cancer. *Cancer Res* 2001;61:2911–2916. [PubMed: 11306467]
- Azad MB, et al. Hypoxia induces autophagic cell death in apoptosis-competent cells through a mechanism involving BNIP3. *Autophagy* 2008;4:195–204. [PubMed: 18059169]
- Beasley NJ, et al. Carbonic anhydrase IX, an endogenous hypoxia marker, expression in head and neck squamous cell carcinoma and its relationship to hypoxia, necrosis, and microvessel density. *Cancer Res* 2001;61:5262–5267. [PubMed: 11431368]
- Bennewith KL, et al. Orally administered pimonidazole to label hypoxic tumor cells. *Cancer Res* 2002;62:6827–6830. [PubMed: 12460894]
- Bozec A, et al. Combined effects of bevacizumab with erlotinib and irradiation: a preclinical study on a head and neck cancer orthotopic model. *Br J Cancer* 2008;99:93–99. [PubMed: 18577994]
- Bristow RG, Hill RP. Hypoxia and metabolism. Hypoxia, DNA repair and genetic instability. *Nat Rev Cancer* 2008;8:180–192. [PubMed: 18273037]
- Brizel DM, et al. Tumor hypoxia adversely affects the prognosis of carcinoma of the head and neck. *Int J Radiat Oncol Biol Phys* 1997;38:285–289. [PubMed: 9226314]
- Brown JM, Giaccia AJ. The unique physiology of solid tumors: opportunities (and problems) for cancer therapy. *Cancer Res* 1998;58:1408–1416. [PubMed: 9537241]
- Bunn HF, Poyton RO. Oxygen sensing and molecular adaptation to hypoxia. *Physiol Rev* 1996;76:839–885. [PubMed: 8757790]
- Cao X, et al. Glucose uptake inhibitor sensitizes cancer cells to daunorubicin and overcomes drug resistance in hypoxia. *Cancer Chemother Pharmacol* 2007;59:495–505. [PubMed: 16906425]
- Cao Y, Klionsky DJ. Physiological functions of Atg6/Beclin 1: a unique autophagy-related protein. *Cell Res* 2007;17:839–849. [PubMed: 17893711]
- Capaccio P, et al. Cyclin D1 expression is predictive of occult metastases in head and neck cancer patients with clinically negative cervical lymph nodes. *Head Neck* 2000;22:234–240. [PubMed: 10748446]
- Carmeliet P, et al. Role of HIF-1alpha in hypoxia-mediated apoptosis, cell proliferation and tumour angiogenesis. *Nature* 1998;394:485–490. [PubMed: 9697772]
- Chapman JD, et al. Measuring hypoxia and predicting tumor radioresistance with nuclear medicine assays. *Radiother Oncol* 1998;46:229–237. [PubMed: 9572615]
- Chaudary N, Hill RP. Hypoxia and metastasis. *Clin Cancer Res* 2007;13:1947–1949. [PubMed: 17404073]

- Chen Z, et al. Metastatic variants derived following in vivo tumor progression of an in vitro transformed squamous cell carcinoma line acquire a differential growth advantage requiring tumor-host interaction. *Clin Exp Metastasis* 1997;15:527–537. [PubMed: 9247255]
- Cuisnier O, et al. Chronic hypoxia protects against gamma-irradiation-induced apoptosis by inducing bcl-2 up-regulation and inhibiting mitochondrial translocation and conformational change of bax protein. *Int J Oncol* 2003;23:1033–1041. [PubMed: 12963983]
- Dalby KN, et al. Targeting the prodeath and prosurvival functions of autophagy as novel therapeutic strategies in cancer. *Autophagy* 2010;6:322–329. [PubMed: 20224296]
- Day GL, Blot WJ. Second primary tumors in patients with oral cancer. *Cancer* 1992;70:14–19. [PubMed: 1606536]
- Dinesman A, et al. Development of a new in vivo model for head and neck cancer. *Otolaryngol Head Neck Surg* 1990;103:766–774. [PubMed: 2126099]
- Eisbruch A, et al. Radiation concurrent with gemcitabine for locally advanced head and neck cancer: a phase I trial and intracellular drug incorporation study. *J Clin Oncol* 2001;19:792–799. [PubMed: 11157033]
- Eisenberg-Lerner A, et al. Life and death partners: apoptosis, autophagy and the cross-talk between them. *Cell Death Differ* 2009;16:966–975. [PubMed: 19325568]
- Evans SM, et al. Detection of hypoxia in human squamous cell carcinoma by EF5 binding. *Cancer Res* 2000;60:2018–2024. [PubMed: 10766193]
- Forastiere A, et al. Head and neck cancer. *N Engl J Med* 2001;345:1890–1900. [PubMed: 11756581]
- Fu KK. Combined-modality therapy for head and neck cancer. *Oncology (Huntingt)* 1997;11:1781–1790. 1796. discussion 1796, 179. [PubMed: 9436185]
- Fu OY, et al. Cobalt chloride-induced hypoxia modulates the invasive potential and matrix metalloproteinases of primary and metastatic breast cancer cells. *Anticancer Res* 2009;29:3131–3138. [PubMed: 19661326]
- Goda N, et al. Hypoxia-inducible factor 1alpha is essential for cell cycle arrest during hypoxia. *Mol Cell Biol* 2003;23:359–369. [PubMed: 12482987]
- Goldberg MA, Schneider TJ. Similarities between the oxygen-sensing mechanisms regulating the expression of vascular endothelial growth factor and erythropoietin. *J Biol Chem* 1994;269:4355–4359. [PubMed: 8308005]
- Haddad RI, Shin DM. Recent advances in head and neck cancer. *N Engl J Med* 2008;359:1143–1154. [PubMed: 18784104]
- Harris AL. Hypoxia--a key regulatory factor in tumour growth. *Nat Rev Cancer* 2002;2:38–47. [PubMed: 11902584]
- Henson B, et al. An orthotopic floor-of-mouth model for locoregional growth and spread of human squamous cell carcinoma. *J Oral Pathol Med* 2007;36:363–370. [PubMed: 17559499]
- Isa AY, et al. Hypoxia in head and neck cancer. *Br J Radiol* 2006;79:791–798. [PubMed: 16854964]
- Janssen HL, et al. Hypoxia in head and neck cancer: how much, how important? *Head Neck* 2005;27:622–638. [PubMed: 15952198]
- Karovic O, et al. Toxic effects of cobalt in primary cultures of mouse astrocytes. Similarities with hypoxia and role of HIF-1alpha. *Biochem Pharmacol* 2007;73:694–708. [PubMed: 17169330]
- Kilic M, et al. Role of hypoxia inducible factor-1 alpha in modulation of apoptosis resistance. *Oncogene* 2007;26:2027–2038. [PubMed: 17043658]
- Kim Y, et al. Hypoxia-regulated delta-like 1 homologue enhances cancer cell stemness and tumorigenicity. *Cancer Res* 2009;69:9271–9280. [PubMed: 19934310]
- Koshikawa N, et al. Hypoxia selects for high-metastatic Lewis lung carcinoma cells overexpressing Mcl-1 and exhibiting reduced apoptotic potential in solid tumors. *Oncogene* 2006;25:917–928. [PubMed: 16247470]
- Koukourakis MI, et al. Beclin 1 over- and underexpression in colorectal cancer: distinct patterns relate to prognosis and tumour hypoxia. *British Journal of Cancer* 2010;103:1209–1214. [PubMed: 20842118]
- Kyasa MJ, et al. Gemcitabine and cisplatin in patients with locally advanced, recurrent, or metastatic head and neck cancer: Results of a Phase II Trial. *The Journal of Applied Research* 2008;8:43–47.

- Le QT. Identifying and targeting hypoxia in head and neck cancer: a brief overview of current approaches. *Int J Radiat Oncol Biol Phys* 2007;69:S56–S58. [PubMed: 17848296]
- Le QT, et al. Galectin-1: a link between tumor hypoxia and tumor immune privilege. *J Clin Oncol* 2005;23:8932–8941. [PubMed: 16219933]
- Levine B, Kroemer G. Autophagy in the pathogenesis of disease. *Cell* 2008;132:27–42. [PubMed: 18191218]
- Liotta LA, Kohn EC. The microenvironment of the tumour-host interface. *Nature* 2001;411:375–379. [PubMed: 11357145]
- Lopez-Albaitero A, Ferris RL. Immune activation by epidermal growth factor receptor specific monoclonal antibody therapy for head and neck cancer. *Arch Otolaryngol Head Neck Surg* 2007;133:1277–1281. [PubMed: 18086972]
- Lorch JH, et al. Induction chemotherapy in locally advanced head and neck cancer: a new standard of care? *Hematol Oncol Clin North Am* 2008;22:1155–1163. viii. [PubMed: 19010265]
- Lukashev D, et al. Hypoxia-dependent anti-inflammatory pathways in protection of cancerous tissues. *Cancer Metastasis Rev* 2007;26:273–279. [PubMed: 17404693]
- Marur S, Forastiere AA. Head and neck cancer: changing epidemiology, diagnosis, and treatment. *Mayo Clin Proc* 2008;83:489–501. [PubMed: 18380996]
- Mashberg A. Diagnosis of early oral and oropharyngeal squamous carcinoma: obstacles and their amelioration. *Oral Oncol* 2000;36:253–255. [PubMed: 10793326]
- Mognetti B, et al. Animal models in oral cancer research. *Oral Oncol* 2006;42:448–460. [PubMed: 16266822]
- Myers JN, et al. An orthotopic nude mouse model of oral tongue squamous cell carcinoma. *Clin Cancer Res* 2002;8:293–298. [PubMed: 11801572]
- Nordsmark M, et al. Prognostic value of tumor oxygenation in 397 head and neck tumors after primary radiation therapy. An international multi-center study. *Radiother Oncol* 2005;77:18–24. [PubMed: 16098619]
- Nordsmark M, et al. Pretreatment oxygenation predicts radiation response in advanced squamous cell carcinoma of the head and neck. *Radiother Oncol* 1996;41:31–39. [PubMed: 8961365]
- Parkin DM, et al. Global cancer statistics. *CA Cancer J Clin* 1999;49:33–64. 1. [PubMed: 10200776]
- Peters LJ. Targeting hypoxia in head and neck cancer. *Acta Oncol* 2001;40:937–940. [PubMed: 11845958]
- Pignon JP, et al. Chemotherapy added to locoregional treatment for head and neck squamous-cell carcinoma: three meta-analyses of updated individual data. MACH-NC Collaborative Group. Meta-Analysis of Chemotherapy on Head and Neck Cancer. *Lancet* 2000;355:949–955. [PubMed: 10768432]
- Piret JP, et al. Hypoxia and CoCl₂ protect HepG2 cells against serum deprivation- and t-BHP-induced apoptosis: a possible anti-apoptotic role for HIF-1. *Exp Cell Res* 2004;295:340–349. [PubMed: 15093734]
- Pitson G, et al. Tumor size and oxygenation are independent predictors of nodal diseases in patients with cervix cancer. *Int J Radiat Oncol Biol Phys* 2001;51:699–703. [PubMed: 11597811]
- Pouyssegur J, et al. Hypoxia signalling in cancer and approaches to enforce tumour regression. *Nature* 2006;441:437–443. [PubMed: 16724055]
- Pursiheimo JP, et al. Hypoxia-activated autophagy accelerates degradation of SQSTM1/p62. *Oncogene* 2009;28:334–344. [PubMed: 18931699]
- Qiu C, et al. A cervical lymph node metastatic model of human tongue carcinoma: Serial and orthotopic transplantation of histologically intact patient specimens in nude mice. *J Oral Maxillofac Surg* 2003;61:696–700. [PubMed: 12796881]
- Qu X, et al. Promotion of tumorigenesis by heterozygous disruption of the beclin 1 autophagy gene. *J Clin Invest* 2003;112:1809–1820. [PubMed: 14638851]
- Reusch U, et al. Anti-CD3 × anti-epidermal growth factor receptor (EGFR) bispecific antibody redirects T-cell cytolytic activity to EGFR-positive cancers in vitro and in an animal model. *Clin Cancer Res* 2006;12:183–190. [PubMed: 16397041]

- Rofstad EK, et al. Fluctuating and diffusion-limited hypoxia in hypoxia-induced metastasis. *Clin Cancer Res* 2007;13:1971–1978. [PubMed: 17360973]
- Roh JL, et al. The prognostic value of hypoxia markers in T2-staged oral tongue cancer. *Oral Oncol* 2009;45:63–68. [PubMed: 18620902]
- Sano D, Myers JN. Xenograft models of head and neck cancers. *Head Neck Oncol* 2009;1:32. [PubMed: 19678942]
- Seiwert TY, Cohen EE. State-of-the-art management of locally advanced head and neck cancer. *Br J Cancer* 2005;92:1341–1348. [PubMed: 15846296]
- Shankaran V, et al. IFN γ and lymphocytes prevent primary tumour development and shape tumour immunogenicity. *Nature* 2001;410:1107–1111. [PubMed: 11323675]
- Siemens DR, et al. Hypoxia increases tumor cell shedding of MHC class I chain-related molecule: role of nitric oxide. *Cancer Res* 2008;68:4746–4753. [PubMed: 18559521]
- Song J, et al. Hypoxia-induced autophagy contributes to the chemoresistance of hepatocellular carcinoma cells. *Autophagy* 2009;5:1131–1144. [PubMed: 19786832]
- Subarsky P, Hill RP. The hypoxic tumour microenvironment and metastatic progression. *Clin Exp Metastasis* 2003;20:237–250. [PubMed: 12741682]
- Sullivan R, Graham CH. Hypoxia-driven selection of the metastatic phenotype. *Cancer Metastasis Rev* 2007;26:319–331. [PubMed: 17458507]
- Swann JB, et al. Demonstration of inflammation-induced cancer and cancer immunoediting during primary tumorigenesis. *Proc Natl Acad Sci U S A* 2008;105:652–656. [PubMed: 18178624]
- Thomas GR, et al. Decreased expression of CD80 is a marker for increased tumorigenicity in a new murine model of oral squamous-cell carcinoma. *Int J Cancer* 1999;82:377–384. [PubMed: 10399955]
- Tredan O, et al. Drug resistance and the solid tumor microenvironment. *J Natl Cancer Inst* 2007;99:1441–1454. [PubMed: 17895480]
- Vaupel P, Mayer A. Hypoxia in cancer: significance and impact on clinical outcome. *Cancer Metastasis Rev* 2007;26:225–239. [PubMed: 17440684]
- Vigneswaran N, et al. Differential susceptibility of metastatic and primary oral cancer cells to TRAIL-induced apoptosis. *Int J Oncol* 2005;26:103–112. [PubMed: 15586230]
- Vordermark D, Brown JM. Endogenous markers of tumor hypoxia predictors of clinical radiation resistance? *Strahlenther Onkol* 2003;179:801–811. [PubMed: 14652668]
- Wan XB, et al. Elevated Beclin 1 expression is correlated with HIF-1 α in predicting poor prognosis of nasopharyngeal carcinoma. *Autophagy* 2010;6:395–404. [PubMed: 20150769]
- Wickramasinghe NS, et al. Hypoxia alters cathepsin B / inhibitor profiles in oral carcinoma cell lines. *Anticancer Res* 2005;25:2841–2849. [PubMed: 16080536]
- Wijffels KI, et al. Tumour cell proliferation under hypoxic conditions in human head and neck squamous cell carcinomas. *Oral Oncol* 2008;44:335–344. [PubMed: 17689286]
- Yan L, et al. Antibody-based therapy for solid tumors. *Cancer J* 2008;14:178–183. [PubMed: 18536557]
- Yan L, et al. Autophagy in chronically ischemic myocardium. *Proc Natl Acad Sci U S A* 2005;102:13807–13812. [PubMed: 16174725]
- Yu Z, et al. Cyclin d1 is a valuable prognostic marker in oropharyngeal squamous cell carcinoma. *Clin Cancer Res* 2005;11:1160–1166. [PubMed: 15709184]
- Yuspa SH, et al. A survey of transformation markers in differentiating epidermal cell lines in culture. *Cancer Res* 1980;40:4694–4703. [PubMed: 7438101]
- Zhang L, Hill RP. Hypoxia enhances metastatic efficiency by up-regulating Mdm2 in KHT cells and increasing resistance to apoptosis. *Cancer Res* 2004;64:4180–4189. [PubMed: 15205329]

**Figure 1.**

Orthotopic murine models of non-metastatic (B4B8) and metastatic (LY2) HNSCC. These murine HNSCC models were established by injecting murine SCC cells B4B8 and LY2 (5×10^6 /mice) submucosally into the mandibular buccal sulcus of Balb/c mice. Extra-oral views (A & C) reveal buccal and submandibular swellings caused by the tumors. The extent of intraoral tumor burden at necropsy was evaluated by gross examination (B and D).

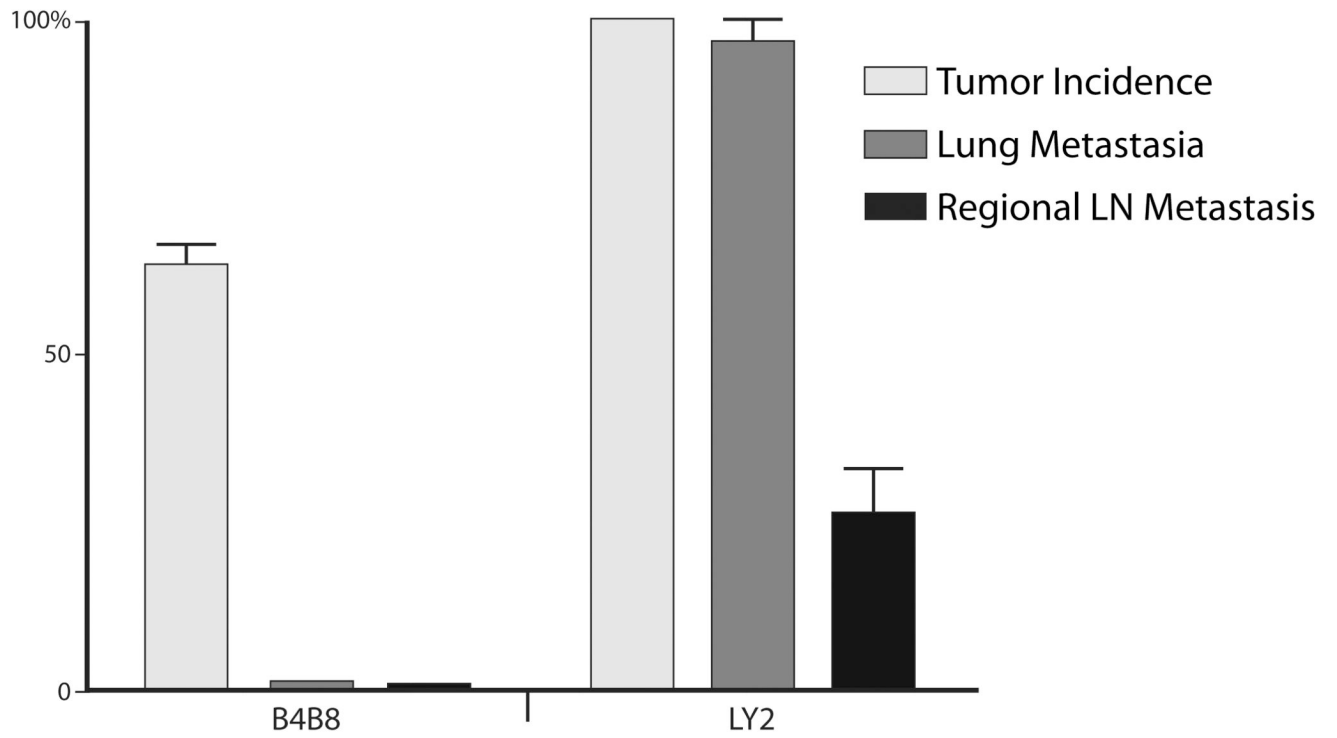


Figure 2. Bar-graph demonstrates the incidences of primary tumor, regional and distant metastases of B4B8 and LY2 tumors.

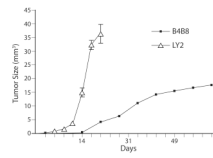


Figure 3. Graphic depiction of the growth rates of B4B8 and LY2 primary tumors. Growth rate of B4B8 tumors is markedly slower than LY2 tumors which become clearly evident approximately one week after tumor cells implantation.

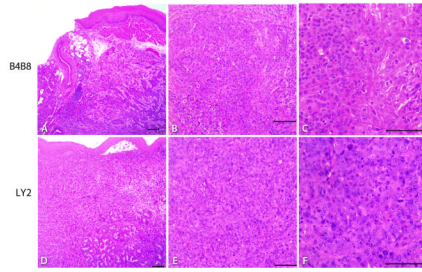


Figure 4.

Representative hematoxylin and eosin stained light microscopy images showing the phenotypic features of B4B8 and LY2 primary tumors. Low power (40 \times) views (A & D) of these tumors reveal invasive islands and cords of malignant squamous cell carcinomas underneath the host's oral mucosal epithelium (bar = 200 μ M). At higher magnifications (100X & 200 \times), B4B8 tumor (B & C) and LY2 tumors (E & F) reveal histopathologic features of well-differentiated low-grade and poorly-differentiated high-grade squamous cell carcinomas, respectively (bar = 100 μ M).

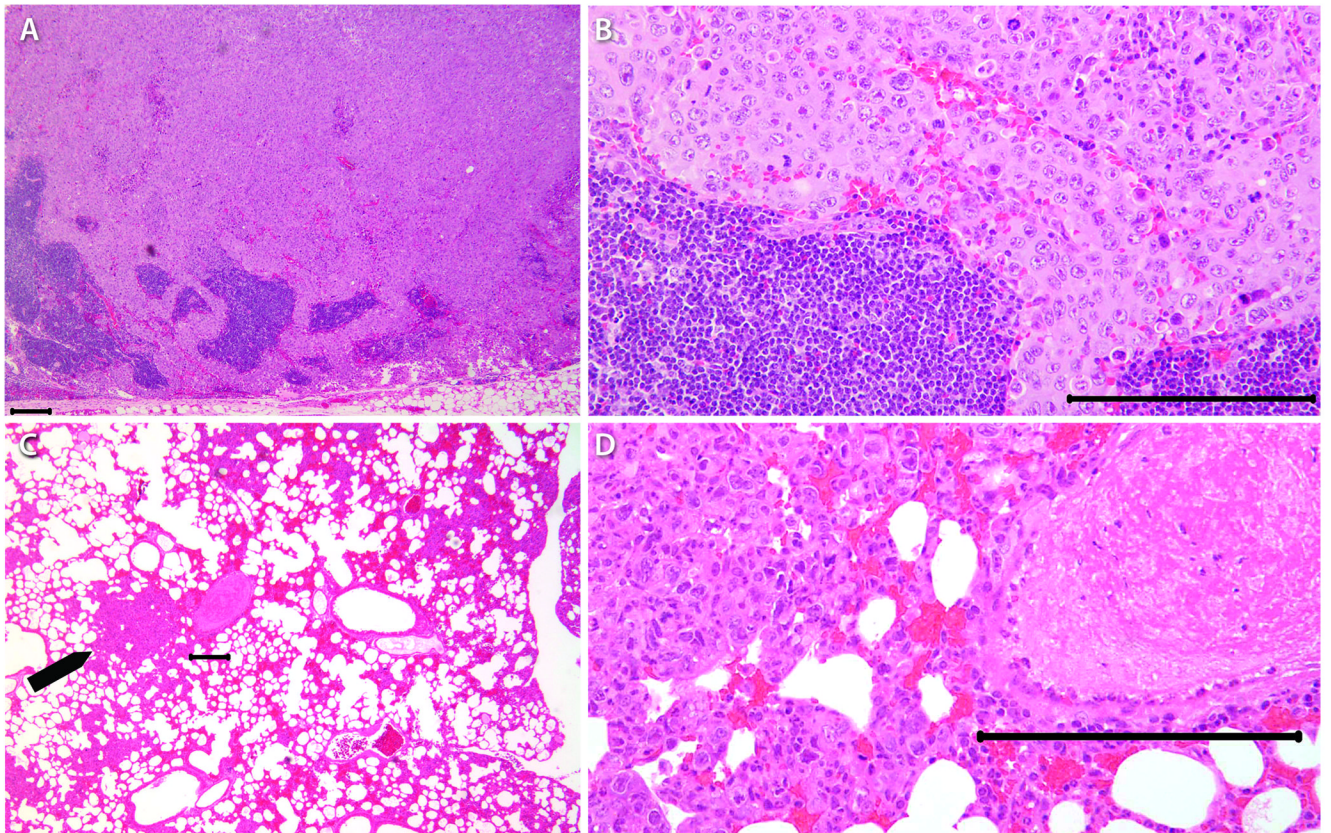


Figure 5. Representative microscopic features of regional lymph nodes and lung with metastatic LY2 tumors. Regional lymph node (A & B) and distant (lung, C & D, arrow) metastases were noted with LY2 tumors but not with B4B8 tumors (bar = 100 μ M).

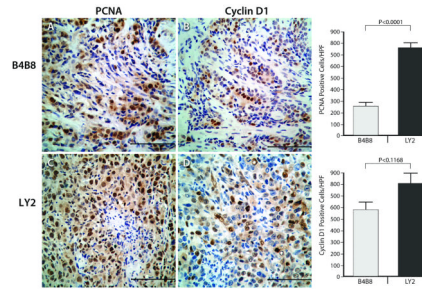


Figure 6.

Representative images of PCNA and cyclin-D1 expression patterns in B4B8 (Top) and LY2 (Bottom) primary tumors. Immunohistochemical staining for PCNA and cyclin-D1 (CyD1) in these tumors shows nuclear reactivity for PCNA and cyclin-D1 and the fraction of tumor cells positive for both of these proliferation markers is markedly higher in LY2 than B4B8 (bar = 100 μ M).

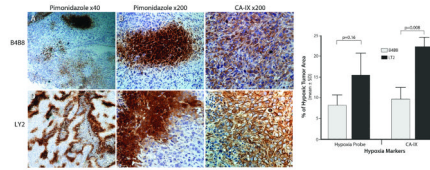


Figure 7.

Representative microscopic images showing the extent of intratumoral hypoxia in B4B8 and LY2 primary tumors. Hypoxic areas in B4B8 and LY2 tumors were identified by pimonidazole binding and CAIX expression patterns. Hypoxic areas as measured by Hypoxyprobe-1 binding and CAIX immunostaining are significantly higher in LY2 primary tumors than B4B8 tumors. Immunohistochemical detection of Hypoxyprobe-1 binding (exogenous marker of hypoxia) and carbonic anhydrase IX (CAIX; endogenous marker of hypoxia) reveal areas of tumor necrosis associated with hypoxia in LY2 tumors but not in B4B8 tumors.

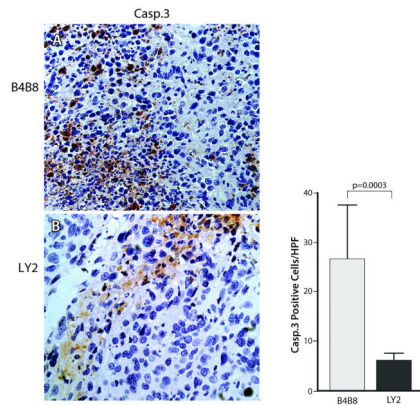


Figure 8.

Detection of apoptosis in hypoxic areas of B4B8 and LY2 tumors by immunelabeling for cleaved caspase 3. Hypoxic areas of B4B8 primary tumor (Top) demonstrate greater number of tumor cells positive for cleaved caspase 3 compared to the hypoxic areas of the LY2 tumor (Bottom). Adjacent bar-graph depicts the mean caspase 3 labeling indices for B4B8 and LY2 tumors in hypoxic areas. Hypoxia-related tumor cells apoptosis rate was significantly higher in B4B8 tumors than that of LY2 tumors.

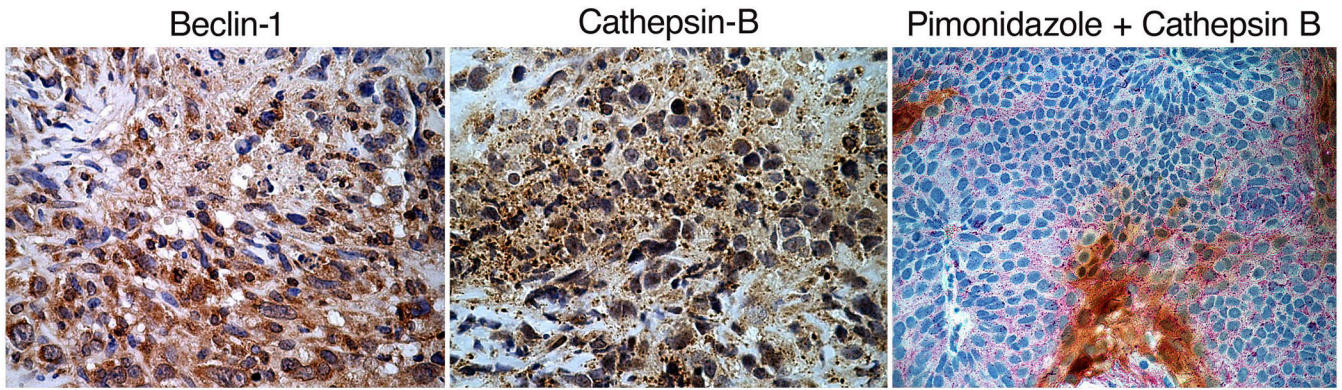


Figure 9.

Detection of autophagic responses in the hypoxic areas of LY2 tumors by immunelabeling for Beclin-1. Hypoxic areas in LY2 primary tumors demonstrate increased expression of Beclin-1 in tumor cells found in the perinecrotic areas. Hypoxic areas of LY2 tumors also exhibit increased expression of lysosomal protease cathepsin B in large granules (phagolysosome). Double immunolabeling for hypoxyprobe-1 (pimonidazole, brown color) and cathepsin B (red color) confirms increased expression of cathepsin B in hypoxic areas of the tumor.

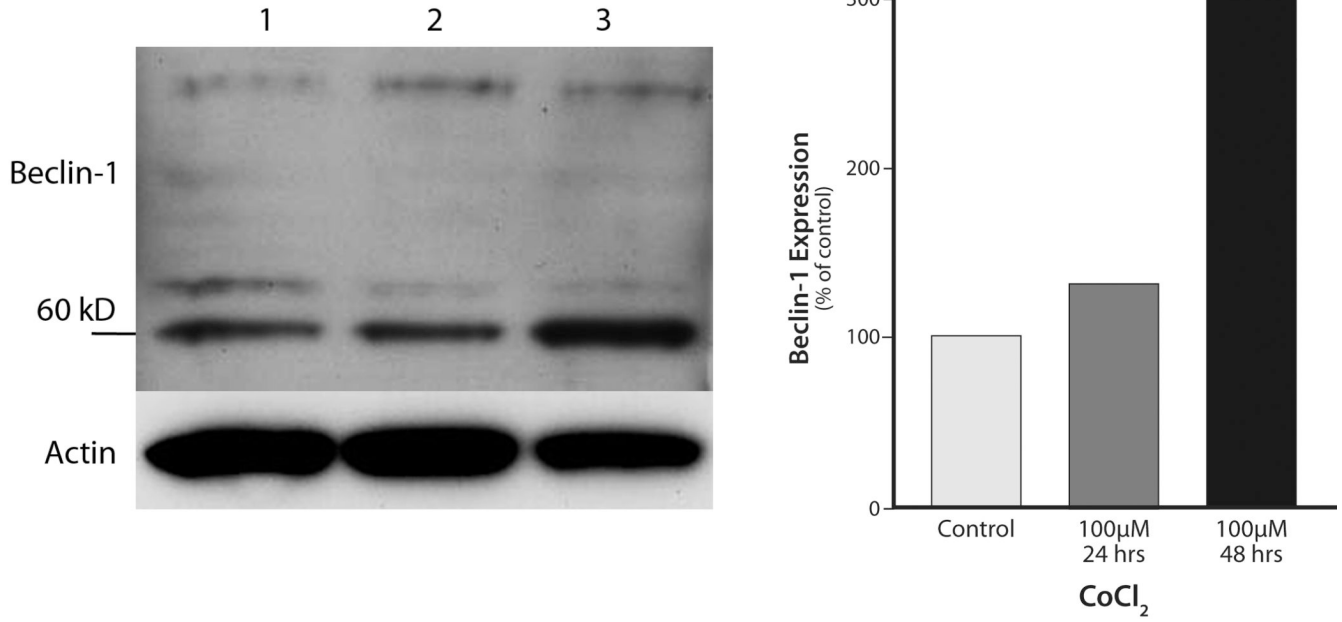


Figure 10.

Immunoblots for Beclin-1 and β -actin expression in LY2 cells treated *in-vitro* with the chemical hypoxia-inducer CoCl₂ (100 μM; 24- & 48-hrs). Hypoxia induction of LY2 cells by CoCl₂ treatment increases expression of autophagic marker Beclin-1. Lanes: 1= control; 2= CoCl₂-24-hrs; 3= CoCl₂-48-hrs.

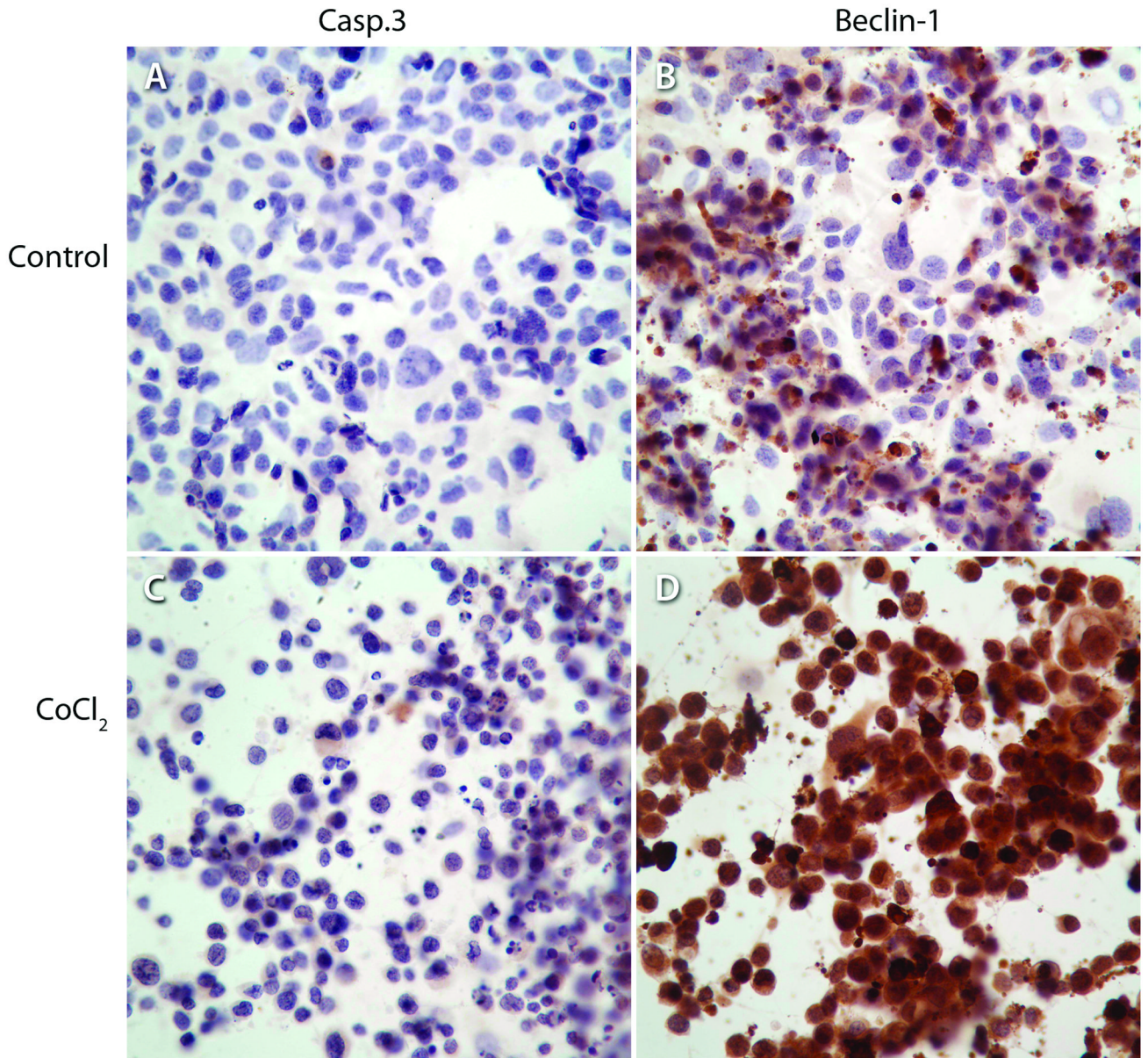


Figure 11.

Immunohistochemical detection of apoptotic marker Casp-3 and autophagic marker Beclin-1 in LY2 cells under normoxic (control) and hypoxic conditions (CoCl₂). Exposure of LY2 cells to hypoxia-mimetic agent (CoCl₂; 100μM; 24-hrs) increases the expression of autophagic marker Beclin-1 and not the apoptotic marker Casp-3.